Front. Optoelectron. China 2009, 2(4): 414–418
DOI 10.1007/s12200-009-0058-0

RESEARCH ARTICLE

Propagation properties of a cylindrically polarized vector beam

Xinting JIA, Bo LI, Youqing WANG (✉), Qing LI, Hongyan HUANG

College of Optoelectronic Science and Engineering, Huazhong University of Science and Technology, Wuhan 430074, China

Abstract A general expression for the electric field of a cylindrically polarized vector beam propagating in free space is derived on the basis of the exact fully vectorial solution of Maxwell equations in transverse Fourier space, which indicates that a cylindrical polarization can be regarded as the combination of radial and azimuthal polarizations, and the electric field retains cylindrical symmetry under the propagation. The simulation results denote that the longitudinal electric field depends on the ratio of the waist width to wavelength and the angle between the electrical vector and the radial direction; in particular, when this angle is 24.5°, a flattop intensity distribution is obtained at the plane $z = 0$.

Keywords cylindrically polarized vector beam, free-space propagation, propagation property, flattop intensity distribution

1 Introduction

Compared with the conventional polarization, a new class of nonuniformly polarized beams, namely, cylindrically polarized beams, is gathering a growing interest recently, which was first introduced by Gori [1]. The cylindrically polarized beam has several unique advantages in physical research and engineering applications due to the cylindrical symmetry of its electrical vector, for example, electron acceleration, particle trapping, high-resolution microscopy, and laser cutting [2–5]. In the case of cylindrical polarization, the angle between the electrical vector and the radial direction is constant on the beam transverse plane, in which radially and azimuthally polarized beams are two particular cases. Various methods for generating cylindrically polarized beams have been reported. For example, Oron et al. obtained radial or azimuthal polarization by combing two linearly polarized TEM_{01} modes with the aid of a discontinuous phase element and a calcite crystal inside the resonator [6]. Niziev et al. used a Sagnac interferometer outside the resonator to generate inhomogeneous polarization [7]. Zhan et al. achieved a generalized cylindrical vector beam from a radially polarized or an azimuthally polarized light by a two-half-wave-plate polarization rotator [8].

The description of a cylindrically polarized vector beam propagating in free space is becoming more and more important due to its unique properties. The standard paraxial theory, neglecting a longitudinal component of the electric field, fails at describing the propagation of a cylindrically polarized vector beam when the beam waist is comparable or even smaller than the wavelength, e.g., a tightly focused beam or laser beam with large divergence angle. Borghi et al. presented the free-space propagation features of the spirally polarized beams in both paraxial and nonparaxial regimes by the vectorial Rayleigh diffraction integral [9].

A new and straightforward treatment is presented for describing the propagation properties of a cylindrically polarized vector beam in free space based on the exact fully vectorial solution of Maxwell equations in transverse Fourier space. The propagation expression derived in this paper indicates that a cylindrically polarized beam can be regarded as the summation of radial and azimuthal polarizations. For a particular angle between the electrical vector and the radial direction, a flattop intensity distribution is formed at the plane $z = 0$.

Received June 10, 2009; accepted June 29, 2009

E-mail: yqwang13@163.com

2 Propagation of a cylindrically polarized vector beam

The transverse electric field distribution of a cylindrically polarized vector beam at the plane $z=0$ reads as

$$\boldsymbol{E}_\perp(r_0,\varphi,0)=\boldsymbol{e}_x E_x(r_0,\varphi,0)+\boldsymbol{e}_y E_y(r_0,\varphi,0), \tag{1}$$

$$E_x(r_0,\varphi,0)=\cos(\varphi+\phi)f(r_0), \tag{2}$$

$$E_y(r_0,\varphi,0)=\sin(\varphi+\phi)f(r_0), \tag{3}$$

where $\boldsymbol{e}_x$ and $\boldsymbol{e}_y$ are the unit vectors in the x and y directions, respectively; r_0 and φ are the polar coordinates; ϕ is a constant angle between the electrical vector and the radial direction; and $f(r_0)$ is a radial function. In this paper, an axially symmetric Laguerre-Gaussian beam of the first order is chosen as the radial function:

$$f(r_0)=\sqrt{2}E_0\frac{r_0}{w_0}\exp\left(-\frac{r_0^2}{w_0^2}\right), \tag{4}$$

where E_0 is an amplitude constant, and w_0 is the waist width of the fundamental mode.

Figure 1 shows the geometry of a cylindrically polarized beam and its electric field over the beam cross section. It is noted that a cylindrically polarized beam has ring intensity distribution, and each point of the beam section is a linear polarization rotated by angle ϕ from its radial direction.

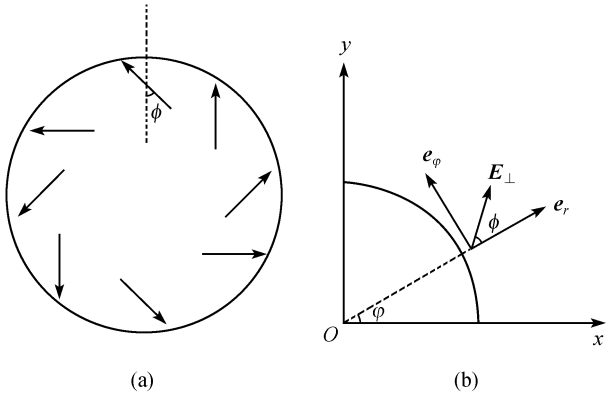

Fig. 1 Geometry of cylindrically polarized beam. (a) Cylindrically polarized beam with angle ϕ between electrical vector and radial direction; (b) transverse electric field of cylindrically polarized beam

The electric field propagating in free space or in a homogeneous medium can be derived by means of the exact fully vectorial solution of Maxwell equations in transverse Fourier space, which gives the electric field in the half-space $z>0$ once its transverse components are known at the plane $z=0$ [10].

$$\boldsymbol{E}(\boldsymbol{r},z)=\iint\exp[\mathrm{i}(\boldsymbol{k}_\perp\cdot\boldsymbol{r}+k_z z)]\cdot\left\{\tilde{\boldsymbol{E}}_\perp(\boldsymbol{k}_\perp)-\left[\frac{\boldsymbol{k}_\perp\cdot\tilde{\boldsymbol{E}}_\perp(\boldsymbol{k}_\perp)}{k_z}\right]\boldsymbol{e}_z\right\}\mathrm{d}^2\boldsymbol{k}_\perp, \tag{5}$$

$$\tilde{\boldsymbol{E}}_\perp(\boldsymbol{k}_\perp)=\frac{1}{(2\pi)^2}\iint\exp(-\mathrm{i}\boldsymbol{k}_\perp\cdot\boldsymbol{r})\boldsymbol{E}_\perp(\boldsymbol{r},0)\mathrm{d}^2\boldsymbol{r}, \tag{6}$$

where $\boldsymbol{e}_z$ is the unit vector in the z direction, $\boldsymbol{r}=x\boldsymbol{e}_x+y\boldsymbol{e}_y$, $\boldsymbol{k}_\perp=k_x\boldsymbol{e}_x+k_y\boldsymbol{e}_y$, $k_z=\sqrt{k^2-k_x^2-k_y^2}$, k is the wave number, and

$$\tilde{\boldsymbol{E}}_\perp(\boldsymbol{k}_\perp)=\tilde{E}_x(\boldsymbol{k}_\perp)\boldsymbol{e}_x+\tilde{E}_y(\boldsymbol{k}_\perp)\boldsymbol{e}_y$$

is the bi-dimensional Fourier transform of the transverse electric field $\boldsymbol{E}_\perp(\boldsymbol{r},0)$. According to Eqs. (1)–(4), Eq. (6) can be written as

$$\begin{cases}\tilde{E}_x(\boldsymbol{k}_\perp)=\mathrm{i}(-\cos\phi k_x+\sin\phi k_y)\\ \qquad\cdot\dfrac{E_0w_0^3}{4\sqrt{2\pi}}\exp\left[-\left(\dfrac{w_0k_\perp}{2}\right)^2\right],\\ \tilde{E}_y(\boldsymbol{k}_\perp)=-\mathrm{i}(\sin\phi k_x+\cos\phi k_y)\\ \qquad\cdot\dfrac{E_0w_0^3}{4\sqrt{2\pi}}\exp\left[-\left(\dfrac{w_0k_\perp}{2}\right)^2\right],\end{cases} \tag{7}$$

where $k_\perp=|\boldsymbol{k}_\perp|$. When the propagation distances are long enough to neglect the effect of the evanescent waves, we consider that $k_\perp$ takes values on the integral interval $[0,k]$. Substitute Eq. (7) into Eq. (5), the following can be obtained:

$$\begin{cases}E_x(\boldsymbol{r},z)=\left(\cos\phi\dfrac{x}{r}-\sin\phi\dfrac{y}{r}\right)\dfrac{\sqrt{2}E_0w_0^3}{4}\displaystyle\int_0^k k_\perp^2\\ \qquad\cdot\exp\left[\mathrm{i}z\sqrt{k^2-k_\perp^2}-\left(\dfrac{w_0k_\perp}{2}\right)^2\right]J_1(rk_\perp)\mathrm{d}k_\perp,\\ E_y(\boldsymbol{r},z)=\left(\cos\phi\dfrac{y}{r}+\sin\phi\dfrac{x}{r}\right)\dfrac{\sqrt{2}E_0w_0^3}{4}\displaystyle\int_0^k k_\perp^2\\ \qquad\cdot\exp\left[\mathrm{i}z\sqrt{k^2-k_\perp^2}-\left(\dfrac{w_0k_\perp}{2}\right)^2\right]J_1(rk_\perp)\mathrm{d}k_\perp,\\ E_z(\boldsymbol{r},z)=\mathrm{i}\cos\phi\dfrac{\sqrt{2}E_0w_0^3}{4}\displaystyle\int_0^k\frac{k_\perp^3}{\sqrt{k^2-k_\perp^2}}\\ \qquad\cdot\exp\left[\mathrm{i}z\sqrt{k^2-k_\perp^2}-\left(\dfrac{w_0k_\perp}{2}\right)^2\right]J_0(rk_\perp)\mathrm{d}k_\perp,\end{cases} \tag{8}$$

where $r=|\boldsymbol{r}|$, $J_0(\cdot)$ and $J_1(\cdot)$ are the zeroth-order and the first-order Bessel functions, respectively. Equation (8) is the basic result obtained in this paper, which describes a cylindrically polarized vector beam propagating in free space.

In the cylindrical coordinate system, the electric field of a cylindrically polarized vector beam is arranged as

$$\begin{cases} \boldsymbol{E}(r,\varphi,z) = E_r(r,\varphi,z)\boldsymbol{e}_r + E_\varphi(r,\varphi,z)\boldsymbol{e}_\varphi + E_z(r,\varphi,z)\boldsymbol{e}_z, \\ E_r(r,\varphi,z) = \cos\phi\dfrac{\sqrt{2}E_0 w_0^3}{4}\displaystyle\int_0^k k_\perp^2 \\ \qquad \cdot\exp\left[\mathrm{i}z\sqrt{k^2-k_\perp^2} - \left(\dfrac{w_0 k_\perp}{2}\right)^2\right]J_1(rk_\perp)\mathrm{d}k_\perp, \\ E_\varphi(r,\varphi,z) = \sin\phi\dfrac{\sqrt{2}E_0 w_0^3}{4}\displaystyle\int_0^k k_\perp^2 \\ \qquad \cdot\exp\left[\mathrm{i}z\sqrt{k^2-k_\perp^2} - \left(\dfrac{w_0 k_\perp}{2}\right)^2\right]J_1(rk_\perp)\mathrm{d}k_\perp, \\ E_z(r,\varphi,z) = \mathrm{i}\cos\phi\dfrac{\sqrt{2}E_0 w_0^3}{4}\displaystyle\int_0^k \frac{k_\perp^3}{\sqrt{k^2-k_\perp^2}} \\ \qquad \cdot\exp\left[\mathrm{i}z\sqrt{k^2-k_\perp^2} - \left(\dfrac{w_0 k_\perp}{2}\right)^2\right]J_0(rk_\perp)\mathrm{d}k_\perp, \end{cases} \tag{9}$$

where

$$\boldsymbol{e}_r = \boldsymbol{e}_x\cos\varphi + \boldsymbol{e}_y\sin\varphi,$$

$$\boldsymbol{e}_\varphi = -\boldsymbol{e}_x\sin\varphi + \boldsymbol{e}_y\cos\varphi.$$

Equation (9) exhibits that a cylindrically polarized beam can be decomposed into radial and azimuthal polarizations, and the electric field retains its cylindrical symmetry under the propagation. When $\phi = 0°$, a cylindrical polarization can degenerate into radial polarization, which includes the radial and longitudinal electric fields; whereas, for $\phi = 90°$, it reduces to azimuthal polarization, and only the azimuthal electric field exists.

For the on-axis case ($x = y = 0$), the electric field of a cylindrically polarized beam is given by

$$\begin{cases} E_x(0,0,z) = 0, \\ E_y(0,0,z) = 0, \\ E_z(0,0,z) = \mathrm{i}\cos\phi\dfrac{\sqrt{2}E_0 w_0^3}{4}\displaystyle\int_0^k \frac{k_\perp^3}{\sqrt{k^2-k_\perp^2}} \\ \qquad \cdot\exp\left[\mathrm{i}z\sqrt{k^2-k_\perp^2} - \left(\dfrac{w_0 k_\perp}{2}\right)^2\right]\mathrm{d}k_\perp. \end{cases} \tag{10}$$

It is easy to find that the transverse component of the electric field on the axis vanishes.

3 Simulation results and discussion

To illustrate the propagation properties of a cylindrically polarized vector beam in detail, numerical simulation has been performed using the formulae derived in Sect. 2. For $\phi = 0°$, the total intensity distributions of a cylindrically polarized vector beam (solid curves)

$$I = |E_x(x,0,z)|^2 + |E_y(x,0,z)|^2 + |E_z(x,0,z)|^2$$

versus x/λ at the plane $z = 100\lambda$ in the cases of $w_0/\lambda = 1.5$ and $w_0/\lambda = 0.8$ are presented in Figs. 2(a) and 2(b), respectively. The corresponding transverse (dotted curves)

$$I_\perp = |E_x(x,0,z)|^2 + |E_y(x,0,z)|^2$$

and longitudinal (dashed curves)

$$I_z = |E_z(x,0,z)|^2$$

intensity distributions versus x/λ are plotted together for comparison. Figure 2(a) denotes that the longitudinal electric field versus the transverse electric field is small. However, with w_0/λ decreasing, there is a noticeable

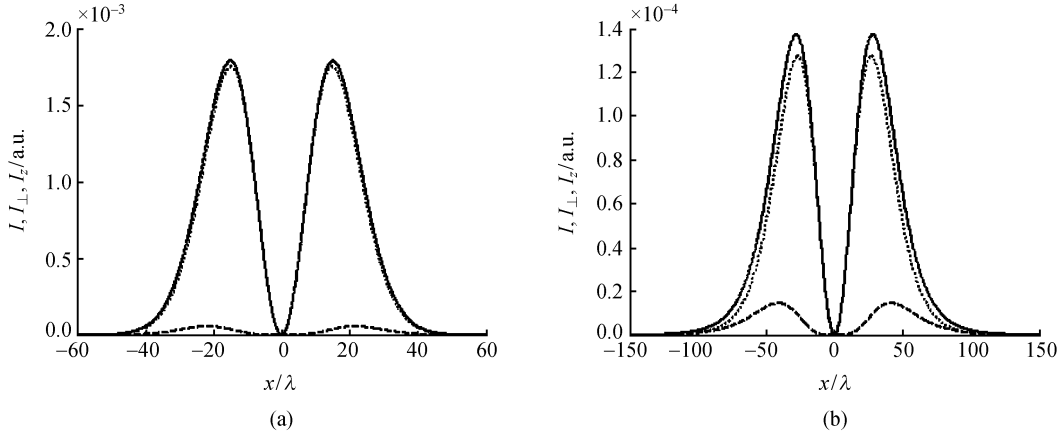

Fig. 2 Total (solid curves), transverse (dotted curves), and longitudinal (dashed curves) intensity distributions of electric field versus x/λ at the plane $z = 100\lambda$ for $\phi = 0°$ in the cases of (a) $w_0/\lambda = 1.5$ and (b) $w_0/\lambda = 0.8$

difference between the total and transverse electric fields due to a large longitudinal electric field, which is shown in Fig. 2(b).

The normalized maximum intensity of the longitudinal electric field $I_{z,\max}/I_{\perp,\max}$ versus w_0/λ at the plane $z=100\lambda$ for $\phi=0°$ is given in Fig. 3. It is easy to find that the longitudinal electric field decreases as w_0/λ increases. When $w_0/\lambda>2.8$, the ratio of $I_{z,\max}/I_{\perp,\max}$ is less than 0.009, which implies that the longitudinal electric field can be neglected. The on-axis longitudinal intensity $I_z(0,0,z)$ versus z/λ at $\phi=0°$ and it versus ϕ at the plane $z=5\lambda$ for different values of $w_0/\lambda=1$ (solid curves), 1.2 (dotted curves), and 1.5 (dashed curves) are depicted in Figs. 4(a) and 4(b), respectively. The intensity of the on-axis longitudinal electric field decreases as the propagation distances and the angle ϕ increase. Particularly, when $\phi=90°$, its intensity is zero for any fixed value of w_0/λ.

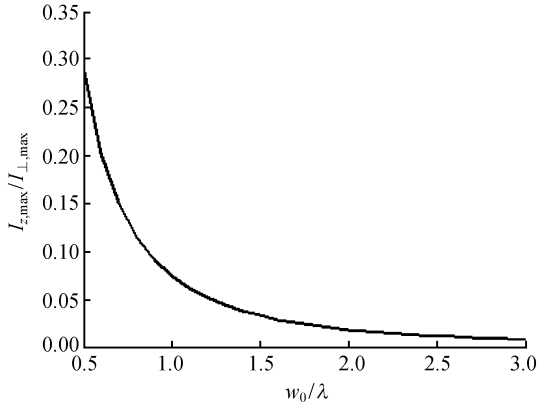

Fig. 3 Normalized maximum intensity of longitudinal electric field versus w_0/λ at the plane $z=100\lambda$ for $\phi=0°$

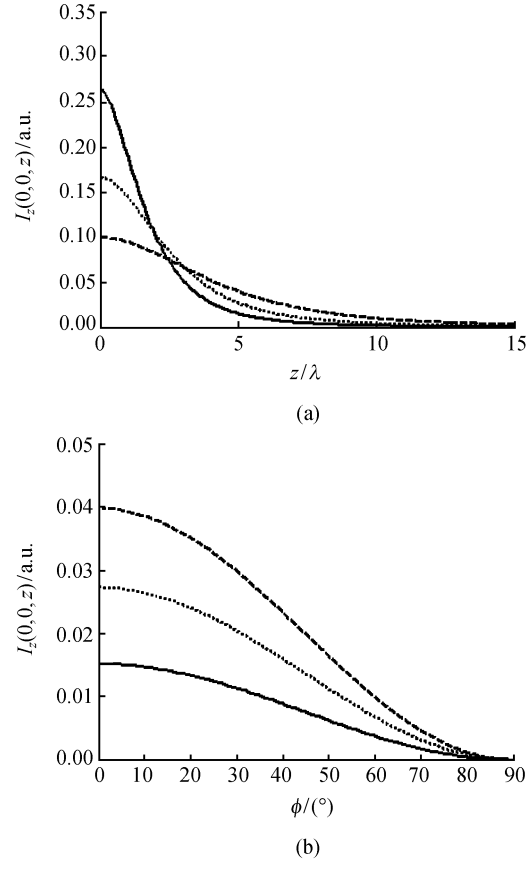

Fig. 4 (a) On-axis longitudinal intensity versus z/λ at $\phi=0°$ and (b) it versus ϕ at the plane $z=5\lambda$ for different values of $w_0/\lambda=1$ (solid curves), 1.2 (dotted curves), and 1.5 (dashed curves)

Figures 3 and 4 indicate that the waist width w_0 and the angle between the electrical vector and the radial direction ϕ have a great impact on the longitudinal electric field. Therefore, it is possible to achieve different profiles of a cylindrically polarized beam by changing the parameters w_0 and ϕ. In the particular case of $\phi=24.5°$, a flattop intensity distribution (solid curve) versus x/λ for $w_0/\lambda=0.8$ at the plane $z=0$ is obtained, as illustrated in Fig. 5. It is noted that the intensity of the transverse electric field (dotted curve) is zero at the center. On the contrary, the longitudinal electric field (dashed curve) has maximum intensity on the beam axis.

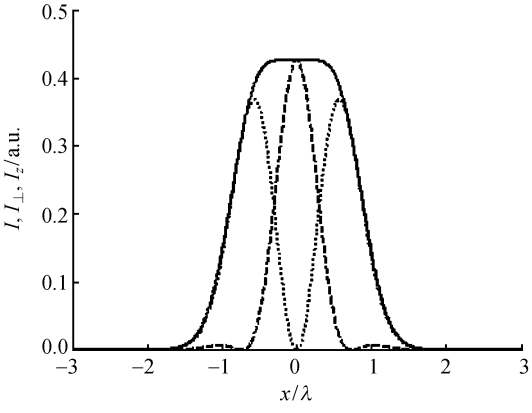

Fig. 5 Total (solid curve), transverse (dotted curve), and longitudinal (dashed curve) intensity distributions of the electric field versus x/λ for $w_0/\lambda=0.8$ at the plane $z=0$ in the case of $\phi=24.5°$ (flattop intensity distribution is obtained)

4 Conclusion

In this study, starting from the exact fully vectorial solution of Maxwell equations in transverse Fourier space, the propagation properties of a cylindrically polarized vector beam in free space have been investigated. A cylindrically polarized beam can be decomposed into radial and azimuthal polarizations. The analyses show that the longitudinal electric field becomes increasingly strong as the ratio of the waist width to wavelength decreases. Various profiles of the cylindrically polarized beam can be formed by adjusting the angle between the electrical vector and the radial direction, particularly when the angle is

24.5°, a flattop intensity distribution is obtained at the plane $z = 0$.

Acknowledgements This work was supported by the National Key Technology Research and Development Program (Grant No. 2007BAF11B01).

References

1. Gori F. Polarization basis for vortex beams. Journal of the Optical Society of America A, 2001, 18(7): 1612–1617
2. Salamin Y I, Keitel C H. Electron acceleration by a tightly focused laser beam. Physical Review Letters, 2002, 88(9): 095005
3. Zhan Q W. Trapping metallic Rayleigh particles with radial polarization. Optics Express, 2004, 12(15): 3377–3382
4. Youngworth K S, Brown T G. Inhomogeneous polarization in scanning optical microscopy. Proceedings of SPIE, 2000, 3919: 75–85
5. Niziev V G, Nesterov A V. Influence of beam polarization on laser cutting efficiency. Journal of Physics D: Applied Physics, 1999, 32 (13): 1455–1461
6. Oron R, Blit S, Davidson N, Friesem A A, Bomzon Z, Hasman E. The formation of laser beams with pure azimuthal or radial polarization. Applied Physics Letters, 2000, 77(21): 3322–3324
7. Niziev V G, Chang R S, Nesterov A V. Generation of inhomogeneously polarized laser beams by use of a Sagnac interferometer. Applied Optics, 2006, 45(33): 8393–8399
8. Zhan Q W, Leger J R. Focus shaping using cylindrical vector beams. Optics Express, 2002, 10(7): 324–331
9. Borghi R, Scantarsiero M. Nonparaxial propagation of spirally polarized optical beams. Journal of the Optical Society of America A, 2004, 21(10): 2029–2037
10. Ciattoni A, Crosignani B, Di Porto P. Vectorial free-space optical propagation: a simple approach for generating all-order nonparaxial corrections. Optics Communications, 2000, 177(1–6): 9–13